Measurement of the conduction band spin-orbit splitting in math xmlns="http://www.w3.org/1998/Math/MathML">msub>mi>WSe/mi>mn>2/mn>/msub>/math> and math xmlns="http://www.w3.org/1998/Math/MathML">msub>mi>WS/mi>mn>2/mn>/msub>/math> monolayers

Lei Ren, Cedric Robert, Hanan Dery, Minhao He, Pengke Li, Dinh Van Tuan, Pierre Renucci, Delphine Lagarde, Takashi Taniguchi, Kenji Watanabe, Xiaodong Xu, and Xavier Marie

Phys. Rev. B **107**, 245407 — Published 6 June 2023

DOI: 10.1103/PhysRevB.107.245407

Measurement of the conduction band spin-orbit splitting in WSe_2 and WS_2 monolayers

Lei Ren,[1,*] Cedric Robert,[1,*] Hanan Dery,[2,3,*] Minhao He,[4] Pengke Li,[2] Dinh Van Tuan,[2] Pierre Renucci,[1] Delphine Lagarde,[1] Takashi Taniguchi,[5] Kenji Watanabe,[6] Xiaodong Xu,[4,7] and Xavier Marie[1,†]

[1] *Université de Toulouse, INSA-CNRS-UPS, LPCNO, 135 Av. Rangueil, 31077 Toulouse, France*
[2] *Department of Electrical and Computer Engineering, University of Rochester, Rochester, New York 14627, USA*
[3] *Department of Physics and Astronomy, University of Rochester, Rochester, New York 14627, USA*
[4] *Department of Physics, University of Washington, Seattle, Washington 98195, USA*
[5] *International Center for Materials Nanoarchitectonics, National Institute for Materials Science, Tsukuba, Ibaraki 305-0044, Japan*
[6] *Research Center for Functional Materials, National Institute for Materials Science, Tsukuba, Ibaraki 305-0044, Japan*
[7] *Department of Materials Science and Engineering, University of Washington, Seattle, Washington 98195, USA*

We have investigated charge tunable devices based on WSe_2 and WS_2 monolayers encapsulated in hexagonal boron nitride. In addition to the well-known radiative recombination of neutral and charged excitons, stationary photoluminescence measurements highlight a weaker intensity optical transition that appears when the monolayer is electrostatically doped with electrons. We have carried out a detailed characterization of this new photoluminescence line based on its doping dependence, its variation as a function of the optical excitation power, its polarization characteristics and its g factor measured under longitudinal magnetic field. We interpret this luminescence peak as an impurity-assisted radiative recombination of the inter-valley negatively charged exciton (triplet trion). In addition to the standard direct recombination, the triplet trion has a second recombination channel triggered by elastic scattering off the short-range impurity potential. The energy difference between the emitted photons from these two possible recombination processes of the same triplet trion is simply the single-particle conduction band spin-orbit splitting Δ_c. We measure $\Delta_c = 12 \pm 0.5$ meV for WSe_2 monolayer and $\Delta_c = 12 \pm 1$ meV for WS_2 monolayer. These results demonstrate the importance of second-order exciton recombination processes in transition-metal dichalcogenide structures.

I. INTRODUCTION

Atomically thin layers of semiconductor transition metal dichalcogenides (TMDs) open up new possibilities for investigation of 2D physics and for potential new applications [1–5]. The band structure is rather unique as a consequence of the large spin-orbit coupling and lack of crystal inversion symmetry of the hexagonal lattice [6]. In addition to the well-known large spin-orbit splitting of the valence bands (VB), the interplay between inversion asymmetry and spin-orbit interaction also yields a smaller spin splitting between the two lowest energy conduction bands (CB) in the K valley, Δ_c [7]. Though this CB spin-orbit splitting has a strong impact on optical, transport and spin-valley properties of TMD monolayers (MLs) [8, 9], its exact value is still poorly known and highly debated. It has been calculated by various groups using ab-initio techniques, yielding scattered results that range from $\Delta_c = -4$ to 40 meV in WSe_2 monolayers [10–12].

From an experimental point of view, optical properties of TMD MLs are dominated by tightly bound excitons [3]. As a consequence, it is not straightforward to determine the single-particle CB spin-orbit splitting from the exciton spectra. Bright and dark neutral excitons are formed with electrons occupying two different CBs with opposite spins in a given K valley. Yet, the measurement of the splitting between these optically active and inactive excitons does not make it possible to determine Δ_c. The reason is that in addition to this spin-orbit splitting, the energy difference between bright and dark excitons depends on the short range electron-hole exchange interaction and the difference in binding energy of the two excitons formed with different electron effective mass [8, 13, 14]. The value of Δ_c in a WSe_2 ML has been estimated recently with an elegant method based on the measurement of the Rydberg series of bright and dark exciton states in a large in-plane magnetic field [15]. Other values of Δ_c have been extracted from transport and optical magneto spectroscopy measurements [16–20], showing scattered results that are influenced by many-body and band-gap renormalization effects in electron or hole rich MLs. A direct and accurate determination of Δ_c is thus highly desirable.

In this work, thanks to the identification of a new line in the photoluminescence (PL) spectra of slightly electron-doped WSe_2 and WS_2 MLs, we have straightforwardly measure $\Delta_c = 12 \pm 0.5$ meV in WSe_2 ML and $\Delta_c = 12 \pm 1$ meV in WS_2 ML. The new PL line we evidenced is interpreted as an impurity-assisted re-

* The first three authors have equal contributions
† marie@insa-toulouse.fr

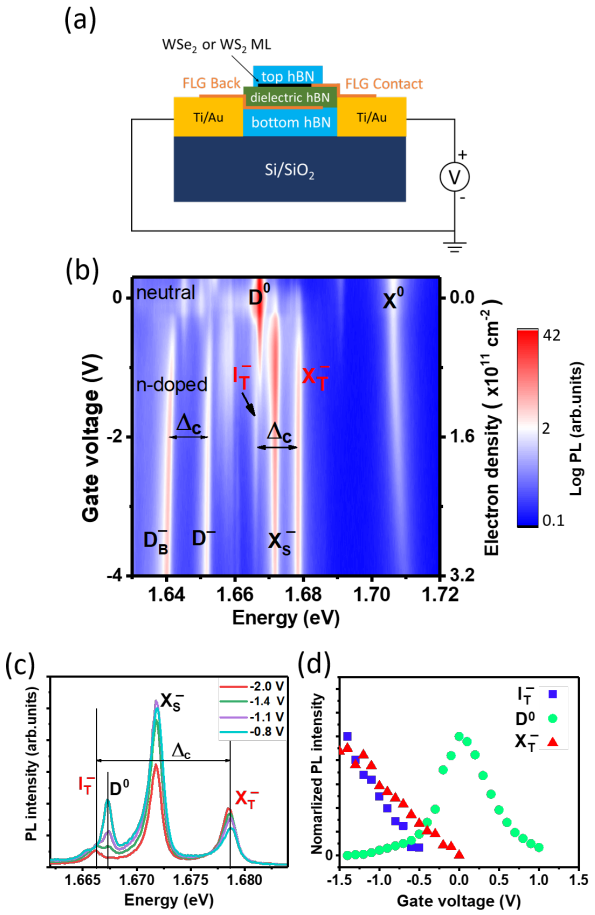

FIG. 1. (a) Sketch of the investigated devices with few layer graphene (FLG) contacts. (b) Photoluminescence intensity in a WSe_2 monolayer as a function of gate voltage (left axis) and corresponding electron density (right axis). The excitation energy is 1.96 eV. Δ_c is the single-particle conduction band spin-orbit splitting. In addition to the relatively weak PL intensity of the peak I_T^-, the spectrum is dominated by emissions from bright and dark neutral excitons (X^0 and D^0), singlet and triplet bright negative trions (X_S^- and X_T^-), and the dark negative trion along with its brightened component (D^- and D_B^-) [8]. (c) The luminescence spectrum at various gate voltages. (d) Voltage dependence of the normalized luminescence intensity for the direct emission from D^0, X_T^-, and I_T^-.

combination of the inter-valley negatively charged exciton (triplet trion), whose radiative recombination energy differs by Δ_c from that of the trion's direct optically active recombination. The organization of this paper is as follows. The samples preparation, PL and magneto-PL measurements are described in Sec. II. Interpretation of the results based on the impurity-assisted recombination mechanism is presented in Sec. III, where we explain the radiative process and detail how to extract Δ_c. Conclusions are given in Sec. IV and the Supplemental Material includes complementary measurement results.

II. EXPERIMENTS

We have fabricated high quality WSe_2 and WS_2 charge adjustable devices as sketched in Fig. 1(a). Details of sample fabrication can be found in Refs. [21, 22]. Electrostatic doping of the ML is controlled by the voltage bias between the back gate and the ML. In the regime of slight to moderate electron density in the ML, the electrons only populate the lowest CBs in both K^+ and K^- valleys (see Fig. 2). A voltage bias change of 1 V in Fig. 1 corresponds typically to an electron density change of 10^{11} cm^{-2} [21]. As shown in Figure S1 of the Supplemental Material [23], the measurements were also performed in another WSe_2 device described in Ref. [26]. Note that in the small doping regime we consider here, the three-particle picture (i.e., trion) and the Fermi-polaron description are equivalent [27, 28]. Continuous wave polarization dependent micro-PL experiments are performed in close cycle cryostats ($T = 4$ K). For WSe_2 and WS_2 devices, the excitation laser wavelengths are 632.8 and 532 nm, respectively. The PL signal is dispersed by a monochromator and detected by a charged-coupled device camera. Magneto-PL experiments in magnetic fields up to 9 T have been carried out in an ultra-stable home-made confocal microscope [29]. Unless otherwise stated, the excitation power is $\sim$5 μW focused to a spot size of $\sim$1 μm diameter.

Three charge tunable WSe_2 devices were fabricated and investigated. As shown in the Supplemental Material, similar results were obtained and here we present the results of one of them. Figure 1(b) presents the PL intensity color plot as a function of applied voltage. In agreement with previous reports, the PL spectra are dominated by the recombination of bright (X^0) and dark (D^0) excitons in the charge-neutral regime, see Figure S2 of the Supplemental Material [23] (the smaller intensity peaks at lower energy correspond to phonon replica [26, 30]). When electrons are added to the ML (negative voltage in our notation) we observe the well identified intravalley (singlet) X_S^- and intervalley (triplet) X_T^- negatively-charged excitons (trions), composed of two electrons and one hole [31]. As shown in Fig. 2(a), the triplet trion is comprised of a photo-generated electron-hole pair, made of an electron in the top CB and a missing electron in the topmost VB of the same valley, and the pair is bound to a resident electron in the bottom CB of the time-reversed valley. The dark trion (D^-) can also be detected in Fig. 1(b) at lower energy [32–35]. The full width at half maximum of X^0 at the charge neutrality point is only 2.5 meV, indicating the high quality of the sample.

A careful reading of Figs. 1(b) and (c) shows that a new line with a rather weak PL intensity appears at 1.666 eV for small negative voltages. This line, labelled I_T^- in the following, is spectrally resolved from the nearby dark exciton (D^0), whose intensity dominates the spectrum when the ML is charge neutral. This PL component (I_T^-) has not been identified so far, though it is present in the PL spectra measured independently by other groups

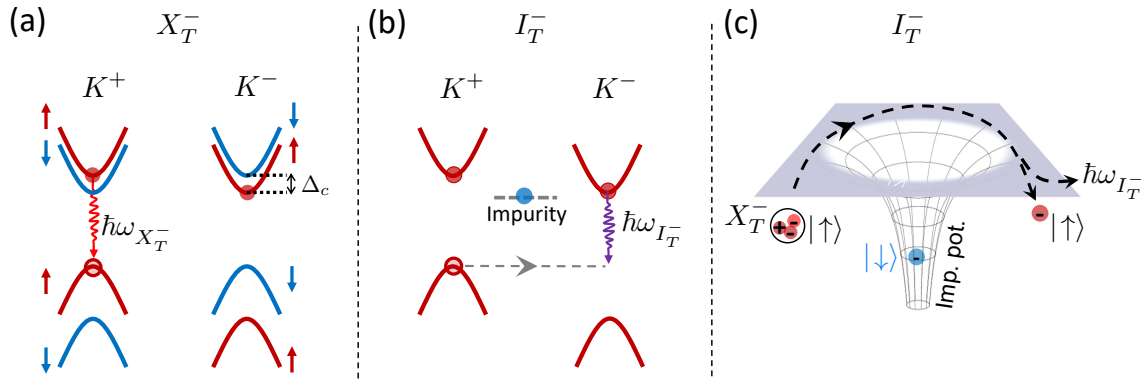

FIG. 2. (a) State composition of the triplet trion in k-space. The initial trion energy is converted to emitted photon, $\hbar\omega_{X_T^-}$, and electron in the bottom valley of K^-. (b) The impurity-assisted recombination process for a triplet trion with spin-up electrons. The hole is transferred to the opposite valley following short-range interaction with the impurity, leading to radiative recombination of the hole with the 'wrong' electron of the trion (i.e., the electron from the opposite valley). The 'horizontal' intervalley transition of the hole represents the elastic nature of the impurity scattering. Using the language of second-order perturbation theory, upon spin-conserving scattering off the impurity, the hole is virtually transferred to the bottom valley of the VB in K^- from which there is strong in-plane dipole transition with the CB bottom valley at K^- . The initial trion energy is converted to the emitted photon energy, $\hbar\omega_{I_T^-}$, and the left behind electron in the top valley of K^+. (c) Schematics of the radiative process in real space. A delocalized triplet trion with two spin-up electrons scatters off an impurity with spin-down localized electron, during which the hole recombines with one of the electrons in the trion. The antiparallel spin configuration of the electrons in the trion and impurity allows the trion to 'touch' the impurity, whereas parallel configuration is forbidden by Pauli exclusion.

on charge adjustable WSe_2 ML devices [26, 36]. We have performed different characterizations in order to identify the origin of this new PL peak.

Figure 1(d) displays the voltage dependence of the normalized PL intensity of the new line I_T^-, as well as the triplet trion (X_T^-) and the neutral dark exciton (D^0). It is clear that this new line emerges when electrons are injected to the ML, while it does not appear when the ML is charge neutral (i.e., when the bright and dark exciton populations dominate). The increase in PL intensity of I_T^- when the electron density increases is very similar to the increase in emission intensity from the triplet trion (X_T^-). With this simple measurement, we already can infer that this line is linked to the recombination of a charged exciton species.

The PL intensity of this new line depends linearly on the excitation power in the typical range between 0.05 and 5 μW (see Figs. S3 and S5 of the Supplemental Material [23]). An interpretation based on multiple exciton complexes, such as charged or neutral biexciton, or localized quantum-dot like states can be ruled out as emission from such states exhibit strongly non-linear behaviors [37–40]. In addition, it turns out that the emission of this line is in-plane polarized. Following the approach detailed in Ref. [41], we selectively filtered the emitted light in angle by imaging the Fourier plane of the microscope objective and by placing a pinhole on this image (Fig. S4 of the Supplemental Material [23]). We find that the emission from I_T^- is not z-polarized, as opposed to the recombination of dark excitons or trions [34, 41].

A decisive argument to identify the new PL line

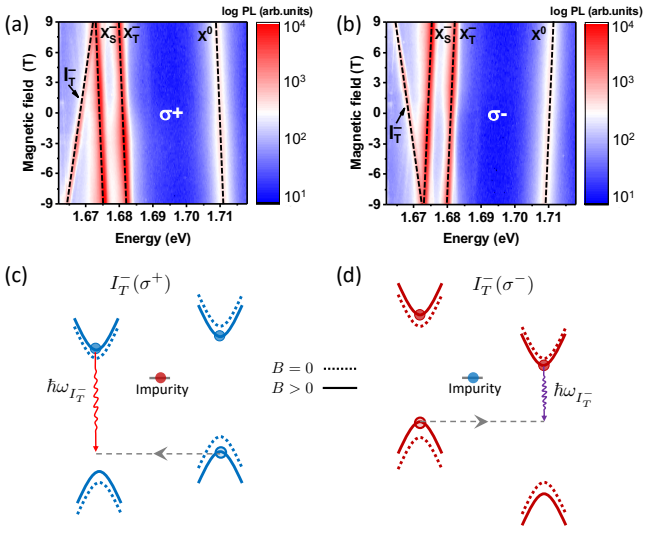

FIG. 3. Magnetic-field dependence of the luminescence in WSe_2 monolayer. The gate voltage is −2 V and the monolayer is excited by a linearly-polarized laser. (a) and (b) show the emitted light detected with σ^+ and σ^- polarizations, respectively. (c) and (d) Schematics of the I_T^- transitions that correspond to emission with $\sigma^\pm$ polarization. The dotted and full lines correspond to energy bands at zero and positive magnetic fields, respectively.

I_T^- is given by magneto-PL measurements presented in Figs. 3(a) and (b). We have recorded the right (σ^+) and left (σ^-) circularly-polarized luminescence spectra for a magnetic field varying between $B = -9$ and +9 T, ap-

plied perpendicularly to the ML plane. The excitation laser is linearly polarized and the gate voltage is −2 V. Absorption or emission of $\sigma^{\pm}$ light occurs in the inequivalent valleys at $K^{\pm}$ of the 2D hexagonal Brillouin zone, as a consequence of the interplay between spin-orbit interaction and lack of inversion symmetry [6, 42–45]. The g factor of a given optical transition with in-plane dipole writes simply, $E_{\sigma^+} - E_{\sigma^-} = g\mu_B B$, where μ_B is the Bohr magneton. As already measured by different groups, we find very similar g factors for both neutral and negatively charged exciton: $g_{X^0} = -4.1 \pm 0.1$, $g_{X_T^-} = -4.4 \pm 0.1$ and $g_{X_S^-} = -4.2 \pm 0.1$ [22, 46–50] . This can be explained by the fact that the optical recombination of these trions involves the same charge carriers in the same valley as for the recombination of the bright neutral exciton, while the spin/valley state of the third carrier in the bottom CB valley is not changed (see for instance Fig. 2(a) for the X_T^- triplet trion recombination).

The striking feature in Fig. 3 is that the slope of the magnetic-field dependent I_T^- line is opposite to the one of the neutral exciton X^0 and the two trion lines X_T^- and X_S^-. The opposite slope means that the g factor of I_T^- is positive. We measure $g_{I_T^-} = +15.4 \pm 0.1$, and find a similar value in the other measured device, shown in Fig. S1 of the Supplemental Material [23]. Note that the line I_T^- does not arise from the recombination of the intervalley dark trion recently identified in WS_2 monolayer. As a matter of fact, it is also characterized by a negative g factor of about −14, opposite to the positive g factor we measured in Fig. 3 [51]. The relatively large amplitude of the measured g factor indicates that the I_T^- transition is governed by indirect recombination of an electron in the bottom CB valley and a hole in the opposite top VB valley [22, 26]. The positive sign of the g factor suggests that the hole experiences intervalley transition, as sketched in Fig. 2(b). The microscopic mechanism which allows the surprising observation of this normally forbidden transition will be detailed in the next section.

Finally, we present the circularly polarized luminescence following circularly polarized laser excitation at zero magnetic field. Figure 4(a) displays the luminescence polarization for singlet and triplet trions, as well as the new line I_T^-. As a consequence of very efficient spin pumping of resident electrons in WSe_2 ML [21], the polarization of the triplet trion reaches very large values up to 80%. In addition, we observe that the polarization of the I_T^- component is also very large, typically 40% and co-polarized with the laser.

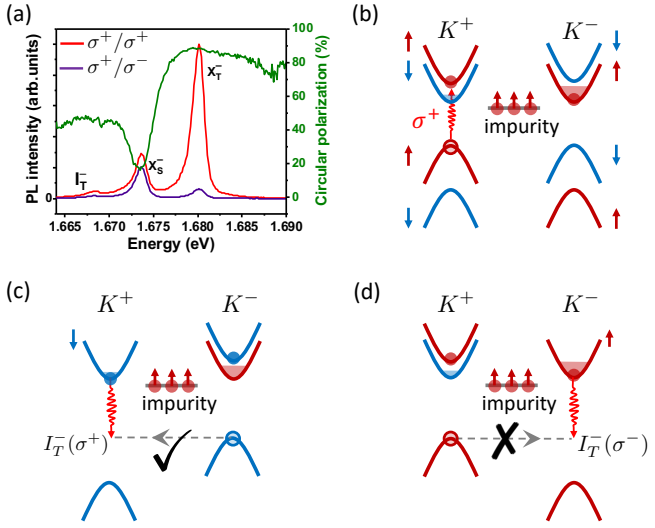

FIG. 4. Polarization analysis of the luminescence in WSe_2 monolayer. The gate voltage is −2 V and the monolayer is excited by a σ^+ polarized laser. (a) PL intensity detected with σ^+ and σ^- polarizations. The green curve displays the corresponding circular polarization degree. (b) schematics of the spin pumping process yielding a spin polarization of resident electrons in the CB valley at K^- and a simultaneous polarization of the impurity electron spin with the same orientation. (c) Due to Pauli exclusion, the short-range scattering of the trion off the impurity occurs only if the two electrons in the trion have opposite spin to that of the impurity electron. (d) The process is inefficient in the other case where the electrons of the trion and impurity have parallel spins. Here, the trion cannot approach the impurity close enough to facilitate intervalley transition of the hole.

III. DISCUSSION

A. Impurity-assisted recombination of the triplet trion

We interpret the I_T^- transition as an impurity-assisted radiative recombination of the triplet trion. As we will show, this mechanism is consistent with the different experimental signatures we described in the previous section. Despite the rather low number of studies on the influence of defects on the properties of TMDs, it is known that WSe_2 or WS_2 monolayers are characterized by a very large density of defects, typically $\sim 10^{12}$ cm^{-2} [52–56]. It has also been shown that chalcogen vacancies induce a significant density of in-gap localized states close to the conduction band [57–59]. These defects induce a strong reduction of the luminescence yield at room temperature but have also some impacts on the recombination channels of certain exciton species. For instance, the zero-phonon indirect exciton transition has been clearly evidenced in WSe_2 monolayer as a consequence of the recombination of an electron and a hole in opposite valleys [26]. In a similar way to the recombination of zero-phonon indirect transitions observed in semiconductors with impurities [60, 61], the respective exciton transition in WSe_2 ML is possible via impurity-assisted recombination, where the large wave-vector mismatch is accommodated by scattering off the short-range part of the impurity potential [30]. An impurity-assisted recombination of intervalley dark trion has also been observed in WS_2 ML [51].

We argue that a similar impurity-assisted recombination process explains the origin of the emission from the peak I_T^-. The initial state is the triplet trion, schematically shown in Fig. 2(a). It is composed of an electron and hole in the top CB and VB valleys at K^+, respectively, which are bound to additional electron in the bottom CB valley at K^-. The photon emission associated to I_T^- is triggered by scattering of the triplet trion off the short-range impurity potential, during which the hole is virtually transitioned to the opposite valley at K^-, as shown schematically in Fig. 2(b). The transferred hole recombines with the resident electron in the opposite valley, emitting a photon with energy $\hbar\omega_{I_T^-}$ and with opposite circular polarization to that of the direct recombination (X_T^-). This recombination process can be described as a second-order transition, in which scattering of the triplet trion off the impurity induces spin-conserving virtual intervalley transition of the hole from the top VB valley at K^+ to the bottom VB valley at K^- (preserving its spin), followed by a virtual type-B optical transition. The transitions are virtual in the sense that the energy of the emitted photon is governed by the initial energy of the triplet and not by the energy gap of the type-B transition. Here, the role of elastic scattering off impurities during recombination is equivalent to the role of the exciton-phonon interaction when dealing with phonon-assisted recombination processes [26, 62, 63].

This interpretation is fully consistent with the magneto-PL results presented in Fig. 3 for linearly-polarized laser excitation. We consider here the lowest energy transitions involving only the top VB, characterized by a g factor g_v. The bottom and top CB g factors are labeled g_{c1} and g_{c2}, respectively. The neutral exciton and trion g factors simply write $g_{X^0} \approx g_{X_T^-} \approx g_{X_S^-} = -2(g_v - g_{c2})$. The exciton g factor measured in Fig. 3 are in good agreement with the recently determined single-particle g factors of the top CB and VB valleys, $g_{c2} = 3.84$ and $g_v = 6.1$ (the g factor of the lowest CB is $g_{c1} = 0.86$) [22].

The impurity-assisted recombination I_T^- of the triplet trion yields a large positive g factor as a consequence of the hole transfer to the opposite valley. Figures 3(c) and (d) show schematics of the CB and VB shifts considering a magnetic field $B > 0$ for σ^+ and σ^- polarized recombination of I_T^-. One can readily check that the energies of these optical transitions simply write:

$$E_{\sigma^\pm} = E_0 \pm (g_v + g_{c1})\mu_B B, \quad (1)$$

yielding a Zeeman splitting energy,

$$\Delta E = E_{\sigma^+} - E_{\sigma^-} = +2(g_v + g_{c1})\mu_B B. \quad (2)$$

Using measured single-particle g factors of the VB and CB [22], the g factor of I_T^- transition is $g_{I_T^-} \approx +13.7$, which is only $\sim 10\%$ smaller than the measured value (+15.4). The impurity-assisted recombination of the triplet trion also explains very well the similar voltage dependence of the luminescence intensity of I_T^- and X_T^- in Fig. 1(d). The two lines correspond to two different recombination channels of the same triplet trion.

The Pauli exclusion principle plays a double role in this impurity-assisted recombination process. First, the electrons of the triplet trion cannot go through a spin-conserving intervalley transition because a trion cannot have two electrons with the same spin and valley. Second, because the radiative process involves short-range scattering off the impurity, the electrons of the trion have to have opposite spin to that of the localized electron in the impurity, as shown in Fig. 2(c). This second feature can explain why the luminescence of the I_T^- line is co-polarized with the laser if we now consider circularly-polarized excitation, as in the experiment presented in Fig. 4. We explain this behavior as follows. As demonstrated in Ref. [21], the σ^+ polarized excitation polarizes the resident electrons in the bottom CB valley at K^-. That is, it results in an imbalance between population of resident electrons in the bottom CB valley at K^+ and K^-, denoted by the shaded areas in Fig. 4(b). The spin pumping process is followed by polarization of the impurity level with similar spin to that of the polarized CB electrons. This kind of impurity spin pumping has been evidenced in various semiconductors [64–67]. The result is that the σ^+ polarized laser yields a spin-up polarization of the impurities, as shown in Figs. 4(c) and (d). Assuming a bimolecular formation of trion from the neutral exciton, we have to consider the two configurations displayed in Figs. 4(c) and (d). These two configurations result from the fact that the neutral exciton polarization is modest (typically 20%, not shown), as a result of the very efficient exciton spin relaxation induced by the long-range electron-hole exchange interaction [68]. Due to Pauli exclusion, short-range scattering off the impurity occurs only in the configuration displayed in Fig. 4(c), where the two electrons spins of the trion are opposite to the impurity's electron spin. Put differently, the spin-up polarized impurity interacts effectively only with triplet trions that have spin-down electrons. The result is σ^+ polarized luminescence (i.e. co-polarized with the laser), in agreement with the experimental results in Fig. 4(a). The scattering of the trion off the impurity with the other configuration, as shown in Fig. 4(d), is inefficient since the two electrons of the trion have parallel spins to that of the impurity.

In summary, the interpretation of the I_T^- transition as an impurity-assisted radiative process of the triplet trion during which the hole recombines with the 'wrong' electron, is consistent with all the experimental characteristics detailed in Sec. II.

1. The emission appears when electrons are added to the ML and its intensity increases in a similar way to the direct-gap emission from the triplet trion, X_T^-.

2. As expected from the second-order recombination process sketched in Fig. 2, the dipole transition is

in-plane polarized and not z-polarized because it involves optical transition between matching spin energy bands.

3. The emission is characterized by a large positive g factor. The large value indicates that the recombination is across the indirect energy gap [26]. The positive value means that the hole experiences intervalley transition, because the Pauli exclusion principle prevents the electrons of a triplet trion from going through an intervalley transition.

4. Following circularly-polarized excitation, the PL circular polarization is co-polarized with the laser one due to spin/valley pumping [21].

We can now understand why triplet and not singlet trions experience impurity-assisted recombination. Any valley switch in the singlet trion case ends up with hole and electron in opposite valleys, which consequently cannot yield emission of any photon. Finally, the screening of the impurity by a large density of free electrons can explain why the emission of I_T^- vanishes when the electron densities are larger than $\sim 3\times10^{11}$ cm^{-2}, in contrast to the direct transition of the triplet X_T^-, as shown in Fig. 1(b).

Alternative interpretations do not make it possible to explain all these experimental facts. For instance, of all phonon-assisted processes, only the K_1 zone-edge phonon replica (18 meV) supports a valley change of the hole to provide a positive g-factor, as measured previously for the neutral indirect exciton or the dark trion [26, 30]. However, this process can be ruled out since no transition exists 18 meV above I_T^-, and furthermore, there should not be a decay of such phonon-assisted emission at larger electron densities. We could also think about a process based on the direct Coulomb interaction between the neutral indirect exciton and resident electrons; this would yield a hole valley change simultaneously with an electron valley change from bottom to top CB valleys. This interpretation could explain the energy position of the I_T^- line and its positive g factor, and yet it is unlikely for two reasons. First, the indirect exciton population is significant only in the neutral region, and it vanishes before the peak I_T^- emerges (in a similar way to the behavior of the dark neutral exciton D^0 in Fig. 1(d)). Second, it was shown theoretically that in these TMD monolayers the exchange scattering is relatively strong despite the neutrality of the exciton, whereas the direct Coulomb scattering component is weak [8]. Finally, we believe that an inelastic scattering process where the trion loses some of its kinetic energy to the screening electron cloud around the impurity can also be ruled out since the experiments are performed at very small charge densities (i.e., no electron screening cloud). Moreover we show that the impurity-assisted recombination effect decays when the screening becomes relevant.

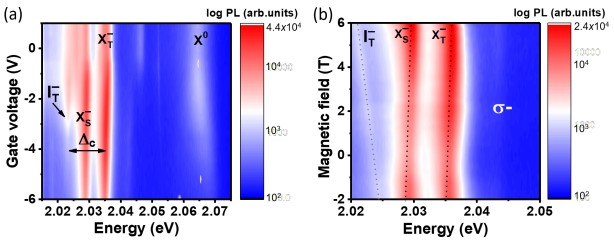

FIG. 5. (a) Photoluminescence intensity as a function of gate voltage in WS_2 monolayer. (b) Magnetic-field dependence of the luminescence for σ^- detection, when the gate voltage is -3 V. The excitation laser energy is 2.33 eV and it is linearly polarized.

B. Measurement of the CB spin-orbit splitting in WSe_2 ML

Compared with the much stronger direct-gap optical transition energy ($\hbar\omega_{X_T^-}$), after which the left-behind electron is the one in the bottom CB valley at K^- (Fig. 2(a)), the left-behind electron in the impurity-assisted recombination process ($\hbar\omega_{I_T^-}$) is the top CB valley electron at K^+ (Fig. 2(b)). Thus, the energy difference between the emitted photons from the two possible recombination processes of the triplet trion is simply the CB spin-orbit splitting (see Figs. 1(b) and (c)). We measure $\Delta_c = 12 \pm 0.5$ meV. Note that the energy difference between the peaks of the triplet trion following regular and impurity-assisted recombination is consistent with the energy difference between the emission of dark trions and their brightened component (labelled D^- and D_{B^-} in Fig. 1(b)). The brightening process of D^- resulting in D_{B^-} has been described in Refs. [8, 9]. In both cases, the energy difference is the CB spin-orbit splitting Δ_c.

The value of Δ_c we determine here is much smaller than the estimated value from measurements of Landau levels in WSe_2 monolayers ($\sim$29 meV) [16]. However, our measured value is consistent with the one estimated from measurement of the Rydberg series of bright and dark excitons in WSe_2 MLs in a large in-plane magnetic field: $\Delta_c \approx 14$ meV [15]. We emphasize that our measurement corresponds to the single-particle CB spin-orbit splitting; it is not influenced by band-gap renormalization effects due to exchnage interactions, as our measurements are performed in relatively small electron densities, of the order of 10^{11} cm^{-2}.

C. Impurity-assisted recombination of the triplet trion and CB spin-orbit splitting in WS_2 ML

All the results presented so far were obtained on WSe_2 ML. We have also investigated a charge adjustable device with WS_2 ML following the exact same approach. As the results are very similar, we will not show all the data and comment only on the main experimental fea-

tures. Figure 5(a) displays the PL intensity color plot as a function of applied voltage in the charge tunable WS_2 device (Fig. S5 of the Supplemental Material shows the power dependence of the PL intensity [23]). Similarly to WSe_2, we recognize the PL peaks associated to the recombination of the bright (X^0) exciton, and when electrons are added to the ML, we recognize the emission from the singlet (X_S^-) and triplet (X_T^-) trions [51, 69, 70]. Remarkably, we also observe the I_T^- line, which has the same characteristics as the one evidenced in WSe_2 ML. Following circularly polarized light excitation, it is co-polarized with the laser and it has a large g factor, $g_{I_T^-} = +14.6 \pm 0.9$, with opposite sign compared to the g factor of the trions, $g_{X_T^-} = -3.5 \pm 0.5$ and $g_{X_S^-} = -3.7 \pm 0.3$, as shown in Fig. 5(b) [71–73]. Using the same reasoning as for WSe_2, the measured difference between the lines X_T^- and I_T^- yields the CB spin-orbit splitting in WS_2 ML. We find $\Delta_c = 12 \pm 1$ meV . The similar values of Δ_c in both WSe_2 and WS_2 MLs, is corroborated by the similarity of other excitonic features (the slightly higher uncertainty for WS_2 is related to broader PL lines). For example, the neutral exciton bright-dark energy splitting is 40 meV in both hBN encapsulated WSe_2 and WS_2 MLs [41, 74].

IV. SUMMARY

We have evidenced a new line in the photoluminescence spectra of WSe_2 and WS_2 monolayers when a relatively small electron density is introduced. The detailed characterizations allowed us to interpret this emission peak as the result of an impurity-assisted recombination of the triplet trion. This identification yields a straightforward measurement of the single-particle conduction band spin-orbit splitting, Δ_c, which is simply the energy difference between the emission peaks of the triplet trion following regular and impurity-assisted recombinations. We find $\Delta_c = 12 \pm 0.5$ meV for WSe_2 monolayer and $\Delta_c = 12 \pm 1$ meV for WS_2 monolayer. Besides the measurement of conduction band spin-orbit splitting, which is key to understand the properties of 2D materials based on transition-metal dichalcogenides, this work shows the importance of second-order recombination processes in WSe_2 or WS_2 monolayers. Phonon or impurity-assisted recombinations could also explain some transitions observed by photoluminescence spectroscopy in hetero- or homo-bilayers.

ACKNOWLEDGMENTS

This work was supported by the Agence Nationale de la Recherche under the program ESR/EquipEx+ (grant number ANR-21-ESRE- 0025) and the ANR projects ATOEMS and Magicvalley. The work at the University of Rochester was supported by the Office of Naval Research (P.L.), under Contract No. N000142112448, and the Department of Energy, Basic Energy Sciences (D.V.T.), under Contract No. DE-SC0014349. The work at University of Washington is supported by the Department of Energy, Basic Energy Sciences, under the award DE-SC0018171.

[1] X. Xu, W. Yao, D. Xiao, and T. F. Heinz, Spin and pseudospins in layered transition-metal dichalcogenides, Nat. Phys. **10**, 343 (2014).

[2] K. F. Mak and J. Shan, Photonics and optoelectronics of 2D semiconductor transition-metal dichalcogenides, Nat. Photon. **10**, 216 (2016).

[3] G. Wang, A. Chernikov, M. M. Glazov, T. F. Heinz, X. Marie, T. Amand, and B. Urbaszek, Colloquium: Excitons in atomically thin transition-metal dichalcogenides, Rev. Mod. Phys. **90**, 021001 (2018).

[4] D. M. Kennes, M. Claassen, L. Xian, A. Georges, A. J. Millis, J. Hone, C. R. Dean, D. N. Basov, A. N. Pasupathy, and A. Rubio, Moiré heterostructures as a condensed-matter quantum simulator, Nat. Phys. **17**, 155 (2021).

[5] E. C. Regan, D. Wang, E. Y. Paik, Y. Zeng, L. Zhang, J. Zhu, A. H. MacDonald, H. Deng, and F. Wang, Emerging exciton physics in transition-metal dichalcogenide heterobilayers, Nat. Rev. Mater. **7**, 778 (2022).

[6] D. Xiao, G.-B. Liu, W. Feng, X. Xu, and W. Yao, Coupled spin and valley physics in monolayers of MoS_2 and other group-VI dichalcogenides, Phys. Rev. Lett. **108**, 196802 (2012).

[7] Y. Song and H. Dery, Transport theory of monolayer transition-metal dichalcogenides through symmetry, Phys. Rev. Lett. **111**, 026601 (2013).

[8] M. Yang ,L. Ren, C. Robert, D. V. Tuan , L. Lombez, B. Urbaszek, X. Marie, and H. Dery, Relaxation and darkening of excitonic complexes in electrostatically doped monolayer WSe_2: Roles of exciton-electron and trion-electron interactions, Phys. Rev. B **105**, 085302 (2022).

[9] D. V. Tuan, S.-F. Shi, X. Xu, S. A. Crooker, and H. Dery, Six-body and eight-body exciton states in monolayer WSe_2, Phys. Rev. Lett. **129**, 076801 (2022).

[10] K. Kośmider, J. W. González, and J. Fernández-Rossier, Large spin splitting in the conduction band of transition metal dichalcogenide monolayers, Phys. Rev. B **88**, 245436 (2013).

[11] A. Kormányos, G. Burkard, M. Gmitra, J. Fabian, V. Zólyomi, N. D. Drummond, and V. Fal'ko, $\mathbf{k}\cdot\mathbf{p}$ theory for two-dimensional transition metal dichalcogenide semiconductors, 2D Mater. **2**, 022001 (2015).

[12] J. P. Echeverry, B. Urbaszek, T. Amand, X. Marie, and I. C. Gerber, Splitting between bright and dark excitons in transition metal dichalcogenide monolayers, Phys. Rev. B **93**, 121107(R) (2016).

[13] D. Y. Qiu, T. Cao, and S. G. Louie, Nonanalyticity, valley quantum phases, and light-like exciton dispersion in monolayer transition metal dichalcogenides: theory and first-principles calculations, Phys. Rev. Lett. **115**, 176801 (2015).

[14] C. Robert, B. Han, P. Kapuscinski, A. Delhomme, C. Faugeras, T. Amand, M. R. Molas, M. Bartos, K. Watanabe, T. Taniguchi, B. Urbaszek, M. Potemski, and X. Marie, Measurement of the spin-forbidden dark excitons in MoS_2 and $MoSe_2$ monolayers, Nat. Commun. **11**, 4037 (2020).

[15] P. Kapuściński, A. Delhomme, D. Vaclavkova, A. O. Slobodeniuk, M. Grzeszczyk, M. Bartos, K. Watanabe, T. Taniguchi, C. Faugeras, and M. Potemski, Rydberg series of dark excitons and the conduction band spin-orbit splitting in monolayer WSe_2, Commun. Phys. **4**, 186 (2021).

[16] Z. Wang, J. Shan, and K. F. Mak, Valley- and spin-polarized Landau levels in monolayer WSe_2, Nat. Nanotechnol. **12**, 144 (2017).

[17] M. V. Gustafsson, M. Yankowitz, C. Forsythe, D. Rhodes, K. Watanabe, T. Taniguchi, J. Hone, X. Zhu, and C. R. Dean, Ambipolar Landau levels and strong band-selective carrier interactions in monolayer WSe_2, Nat. Mater. **17**, 411 (2018).

[18] R. Pisoni, A. Kormányos, M. Brooks, Z. Lei, P. Back, M. Eich, H. Overweg, Y. Lee, P. Rickhaus, K. Watanabe, T. Taniguchi, A. Imamoglu, G. Burkard, T. Ihn, and K. Ensslin, Interactions and magneto-transport through spin-valley coupled Landau levels in monolayer MoS_2, Phys. Rev. Lett. **121**, 247701 (2018).

[19] Y. Wang, T. Sohier, K. Watanabe, T. Taniguchi, M. J. Verstraete, and E. Tutuc, Electron mobility in monolayer WS_2 encapsulated in hexagonal boron-nitride, Appl. Phys. Lett. **118**, 102105 (2021).

[20] S. Larentis, H. C. P. Movva, B. Fallahazad, K. Kim, A. Behroozi, T. Taniguchi, K. Watanabe, S. K. Banerjee, and E. Tutuc, Large effective mass and interaction-enhanced Zeeman splitting of K-valley electrons in $MoSe_2$, Phys. Rev. B **97**, 201407 (2018).

[21] C. Robert, S. Park, F. Cadiz, L. Lombez, L. Ren, H. Tornatzky, A. Rowe, D. Paget, F. Sirotti, M. Yang, D. V. Tuan, T. Taniguchi, B. Urbaszek, K. Watanabe, T. Amand, H. Dery, and X. Marie, Spin/Valley pumping of resident electrons in WSe_2 and WS_2 monolayers, Nat. Commun. **12**, 5455 (2021).

[22] C. Robert, H. Dery, L. Ren, D. Van Tuan, E. Courtade, M. Yang, B. Urbaszek, D. Lagarde, K. Watanabe, T. Taniguchi, T. Amand, and X. Marie, Measurement of conduction and valence bands g-factors in a transition metal dichalcogenide monolayer, Phys. Rev. Lett. **126**, 067403 (2021).

[23] See Supplemental Material at `http://link.aps.org/...` for details on the magneto-PL measurement of I_T^- performed in a second WSe_2 device, and measurements of the dipole orientation as well as power dependence in WSe_2 and WS_2 devices. The Supplemental Material includes Refs. [24]-[25].

[24] Z. Wang, L. Zhao, K. F. Mak, and J. Shan, Probing the spin-polarized electronic band structure in monolayer transition metal dichalcogenides by optical spectroscopy, Nanolett. **17**, 740 (2017).

[25] J. Li, M. Goryca, K. Yumigeta, H. Li, S. Tongay, and S. A. Crooker, Valley relaxation of resident electrons and holes in a monolayer semiconductor: Dependence on carrier density and the role of substrate-induced disorder, Phys. Rev. Mat. **5**, 044001(2021).

[26] M. He, P. Rivera, D. V. Tuan, N. P. Wilson, M. Yang, T. Taniguchi, K. Watanabe, J. Yan, D. G. Mandrus, H. Yu, H. Dery, W. Yao, and X. Xu, Valley phonons and exciton complexes in a monolayer semiconductor, Nat. Commun. **11**, 618 (2020).

[27] M. Sidler, P. Back, O. Cotlet, A.Srivastava, T. Fink, M. Kroner, E. Demler, and A. Imamoglu, Fermi polaron-polaritons in charge-tunable atomically thin semiconductors, Nat. Phys. **13**, 255 (2017).

[28] M. M. Glazov, Optical properties of charged excitons in two-dimensional semiconductors, J. Chem. Phys. **153**, 034703 (2020).

[29] T. Belhadj, C.-M. Simon, T. Amand, P. Renucci, B. Chatel, O. Krebs, A. Lemaitre, P. Voisin, X. Marie, and B. Urbaszek, Controlling the polarization eigenstate of a quantum dot exciton with light, Phys. Rev. Lett. **103**, 086601 (2009).

[30] P. Li, C. Robert, D. Van Tuan, L. Ren, M. Yang, X. Marie, and H. Dery, Intervalley electron-hole exchange interaction and impurity-assisted recombination of indirect excitons in WS_2 and WSe_2 monolayers, Phys. Rev. B **106**, 085414 (2022).

[31] A. M. Jones, H. Yu, J. Schaibley, J. Yan, D. G. Mandrus, T. Taniguchi, K. Watanabe, H. Dery, W. Yao, and X. Xu, Excitonic luminescence upconversion in a two-dimensional semiconductor, Nat. Phys. **12**, 323 (2016).

[32] E. Courtade, M. Semina, M. Manca, M. M. Glazov, C. Robert, F. Cadiz, G. Wang, T. Taniguchi, K. Watanabe, M. Pierre, W. Escoffier, E. L. Ivchenko, P. Renucci, X. Marie, T. Amand, and B. Urbaszek, Charged excitons in monolayer WSe_2: experiment and theory, Phys. Rev. B **96**, 085302 (2017).

[33] Z. Li, T. Wang, S. Miao, Z. Lian, and S.-F. Shi, Fine structures of valley-polarized excitonic states in monolayer transitional-metal dichalcogenides, Nanophotonics **9**, 1811 (2020).

[34] E. Liu, J. van Baren, Z. Lu, M. M. Altaiary, T. Taniguchi, K. Watanabe, D. Smirnov, and C. H. Lui, Gate tunable dark trions in monolayer WSe_2, Phys. Rev. Lett. **123**, 027401 (2019).

[35] Z. Li, T. Wang, Z. Lu, M. Khatoniar, Z. Lian, Y. Meng, M. Blei, T. Taniguchi, K. Watanabe, S. A. McGill, S. Tongay, V. M. Menon, D. Smirnov, and S.-F. Shi, Direct observation of gate-tunable dark trions in monolayer WSe_2, Nano Lett. **19**, 6886 (2019).

[36] E. Liu, J. van Baren, C.-T. Liang, T. Taniguchi, K. Watanabe, N. M. Gabor, Y.-C. Chang, and C.-H. Lui, Multipath optical recombination of intervalley dark excitons and trions in monolayer WSe_2, Phys. Rev. Lett. **124**, 196802 (2020).

[37] M. Barbone, A. R.-P. Montblanch, D. M. Kara, C. Palacios-Berraquero, A. R. Cadore, D. De Fazio, B. Pingault, E. Mostaani, H. Li, B. Chen, K. Watanabe, T. Taniguchi, S. Tongay, G. Wang, A. C. Ferrari, and M. Atatüre , Charge-tuneable biexciton complexes in monolayer WSe_2, Nat. Commun. **9**, 3721 (2018).

[38] A. Srivastava, M. Sidler, A. V. Allain, D. S. Lembke, A. Kis, and A. Imamoglu, Optically active quantum dots in monolayer WSe_2, Nat. Nanotechnol. **10**, 491 (2015).

[39] Y.-M. He, G. Clark, J. R. Schaibley, Y. He, M.-C. Chen, Y.-J. Wei, X. Ding, Q. Zhang, W. Yao, X. Xu, C.-Y. Lu, and J.-W. Pan, Single quantum emitters in monolayer

semiconductors, Nat. Nanotechnol. **10**, 497 (2015).
[40] M. Koperski, K. Nogajewski, A. Arora, V. Cherkez, P. Mallet, J.-Y. Veuillen, J. Marcus, P. Kossacki, and M. Potemski, Single photon emitters in exfoliated WSe_2 structures, Nat. Nanotechnol. **10**, 503 (2015).
[41] G. Wang, C. Robert, M. M. Glazov, F. Cadiz, E. Courtade, T. Amand, D. Lagarde, T. Taniguchi, K. Watanabe, B. Urbaszek, and X. Marie, In-plane propagation of light in transition metal dichalcogenide monolayers: optical selection rules, Phys. Rev. Lett. **119**, 047401 (2017).
[42] G. Sallen, L. Bouet, X. Marie, G. Wang, C. R. Zhu, W. P. Han, Y. Lu, P. H. Tan, T. Amand, B. L. Liu, and B. Urbaszek, Robust optical emission polarization in MoS_2 monolayers through selective valley excitation, Phys. Rev. B **86**, 081301(R) (2012).
[43] K. F. Mak, K. L. He, J. Shan, and T. F. Heinz, Control of valley polarization in monolayer MoS_2 by optical helicity, Nat. Nanotechnol. **7**, 494 (2012).
[44] T. Cao, G. Wang, W. Han, H. Ye, C. Zhu, J. Shi, Q. Niu, P. Tan, E. Wang, B. Liu, and J. Feng, Valley-selective circular dichroism of monolayer molybdenum disulphide, Nat. Commun. **3**, 887 (2012).
[45] G. Kioseoglou, A. T. Hanbicki, M. Currie, A. L. Friedman, D. Gunlycke, and B. T. Jonker, Valley polarization and intervalley scattering in monolayer MoS_2, Appl. Phys. Lett. **101**, 221907 (2012).
[46] G. Wang, L. Bouet, M. M. Glazov, T. Amand, E. L. Ivchenko, E. Palleau, X. Marie, and B. Urbaszek, Magneto-optics in transition-metal diselenide monolayers, 2D Mater. **2**, 034002 (2015).
[47] G. Aivazian, Z. Gong, A. M. Jones, R.-L. Chu, J. Yan, D. G. Mandrus, C. Zhang, D. Cobden, W. Yao, and X. Xu, Magnetic control of valley pseudospin in monolayer WSe_2, Nat. Phys. **11**, 148 (2015).
[48] A. Srivastava, M. Sidler, A. V. Allain, D. S. Lembke, A. Kis, and A. Imamoglu, Valley Zeeman effect in elementary optical excitations of monolayer WSe_2, Nat. Phys. **11**, 141 (2015).
[49] C. Robert, T. Amand, F. Cadiz, D. Lagarde, E. Courtade, M. Manca, T. Taniguchi, K. Watanabe, B. Urbaszek, and X. Marie, Fine structure and lifetime of dark excitons in transition metal dichalcogenide monolayers, Phys. Rev. B **96**, 155423 (2017).
[50] M. R. Molas, A. O. Slobodeniuk, T. Kazimierczuk, K. Nogajewski, M. Bartos, P. Kapuciski, K. Oreszczuk, K. Watanabe, T. Taniguchi, C. Faugeras, P. Kossacki, D. M. Basko, M. Potemski, Probing and manipulating valley coherence of dark excitons in monolayer WSe_2, Phys. Rev. Lett. **123**, 096803 (2019).
[51] M. Zinkiewicz, T. Woźniak, T. Kazimierczuk, P. Kapuscinski, K. Oreszczuk, M. Grzeszczyk, M. Bartos, K. Nogajewski, K. Watanabe, T. Taniguchi, C. Faugeras, P. Kossacki, M. Potemski, A. Babiński, and M. R. Molas, Excitonic complexes in n-doped WS_2 monolayer, Nano Lett. **21**, 2519 (2021).
[52] M. R. Molas, K. Nogajewski, A. O. Slobodeniuk, J. Binder, M. Bartos, and M. Potemski, The optical response of monolayer, few-layer and bulk tungsten disulfide, Nanoscale **9**, 13128 (2017).
[53] D. Edelberg, D. Rhodes, A. Kerelsky, B. Kim, J. Wang, A. Zangiabadi, C. Kim, A. Abhinandan, J. Ardelean, M. Scully, D. Scullion, L. Embon, R. Zu, E. J. G. Santos, L. Balicas, C. Marianetti, K. Barmak, X. Zhu, J. Hone, and A. N. Pasupathy, Approaching the intrinsic limit in transition-metal diselenides via point defect control, Nano Lett. **19**, 4371 (2019).
[54] A. Neumann, J. Lindlau, M. Nutz, A. D. Mohite, H. Yamaguchi, and A. Högele, Signatures of defect-localized charged excitons in the photoluminescence of monolayer molybdenum disulfide, Phys. Rev. Mater. **2**, 124003 (2018).
[55] D. Rhodes, S. H. Chae, R. Ribeiro-Palau, and J. Hone, Disorder in van Der Waals heterostructures of 2D materials, Nat. Mater. **18**, 541 (2019).
[56] W. Murray, M. Lucking, E. Kahn, T. Zhang, K. Fujisawa, N. Perea-Lopez, A. L. Elias, H. Terrones, M. Terrones, and Z. Liu, Second harmonic generation in two-dimensional transition metal dichalcogenides with growth and post-synthesis defects, 2D Mater. **7**, 045020 (2020).
[57] S. Refaely-Abramson, D. Y. Qiu, S. G. Louie, and J. B. Neaton, Defect-induced modification of low-lying excitons and valley selectivity in monolayer transition-metal dichalcogenides, Phys. Rev. Lett. **121**, 167402 (2018).
[58] H. Bretscher, Z. Li, J. Xiao, D. Y. Qiu , S. Refaely-Abramson, J. A. Alexander-Webber, A. Tanoh, Y. Fan, G. Delport, C. A. Williams, S. D. Stranks, S. Hofmann, J. B. Neaton, S. G. Louie, and A. Rao , Rational passivation of sulfur vacancy defects in two-dimensional transition metal dichalcogenides, ACS Nano **15**, 8780 (2021).
[59] P. Rivera, M. He, B. Kim, S. Liu, C. Rubio-Verdú, H. Moon, L. Mennel, D. A. Rhodes, H. Yu, T. Taniguchi, K. Watanabe, J. Yan, D. G. Mandrus, H. Dery, A. Pasupathy, D. Englund, J. Hone, W. Yao, and X. Xu, Intrinsic donor-bound excitons in ultraclean monolayer semiconductors, Nat. Commun. **12**, 871 (2021).
[60] M. Tajima, Determination of boron and phosphorus concentration in silicon by photoluminescence analysis, Appl. Phys. Lett. **32**, 719 (1978).
[61] J. Wagner, Heavily doped silicon studied by luminescence and selective absorption, Sol. Stat. Electron. **28**, 25 (1985).
[62] H. Dery and Y. Song, Polarization analysis of excitons in monolayer and bilayer transition-metal dichalcogenides, Phys. Rev. B **92**, 125431 (2015).
[63] D. Van Tuan, A. M. Jones, M. Yang, X. Xu, and H. Dery, Virtual trions in the photoluminescence of monolayer transition-metal dichalcogenides, Phys. Rev. Lett. **122**, 217401 (2019).
[64] V. L. Berkovits, A. I. Ekimov, and V. I. Safarov, Optical orientation in a system of electrons and lattice nuclei in semiconductors. Experiment, Sov. Phys. JETP **38**, 169 (1974).
[65] M. I. D'yakonov and V. I. Perel, Optical orientation in a system of electrons and lattice nuclei in semiconductors. Theory, Sov. Phys. JETP **38**, 177 (1974).
[66] Q. Liu, C.-X. Liu, C. Xu, X.-L. Qi, and S.-C. Zhang, Magnetic impurities on the surface of a topological insulator, Phys. Rev. Lett. **102**, 156603 (2009).
[67] L. Qing, J. Li, I. Appelbaum, and H. Dery, Spin relaxation via exchange with donor impurity-bound electrons, Phys. Rev. B **91**, 241405 (2015).
[68] C. R. Zhu, K. Zhang, M. Glazov, B. Urbaszek, T. Amand, Z. W. Ji, B. L. Liu, and X. Marie, Exciton valley dynamics probed by Kerr rotation in WSe_2 monolayers, Phys. Rev. B **90**, 161302 (2014).
[69] D. Vaclavkova, J. Wyzula, K. Nogajewski, M. Bartos, A. O. Slobodeniuk, C. Faugeras, M. Potemski, and M. R.

Molas, Singlet and triplet Trions in WS_2 monolayer encapsulated in hexagonal boron nitride, Nanotechnology **29**, 325705 (2018).

[70] A. Arora, N. K. Wessling, T. Deilmann, T. Reichenauer, P. Steeger, P. Kossacki, M. Potemski, S. Michaelis de Vasconcellos, M. Rohlfing, and R. Bratschitsch, Dark trions govern the temperature-dependent optical absorption and emission of doped atomically thin semiconductors, Phys. Rev. B **101**, 241413 (2020).

[71] R. Schmidt, A. Arora, G. Plechinger, P. Nagler, A. Granados del Aguila, M. V. Ballottin, P. C. M. Christianen, S. M. de Vasconcellos, C. Schüller, T. Korn, and R. Bratschitsch, Magnetic-field-induced rotation of polarized light emission from monolayer WS_2, Phys. Rev. Lett. **117**, 077402 (2016).

[72] P. Nagler, M. V. Ballottin, A. A. Mitioglu, M. V. Durnev, T. Taniguchi, K. Watanabe, A. Chernikov, C. Schüller, M. M. Glazov, P. C. M. Christianen, and T. Korn, Zeeman splitting and inverted polarization of biexciton emission in monolayer WS_2, Phys. Rev. Lett. **121**, 057402 (2018).

[73] M. Koperski, M. R. Molas, A. Arora, K. Nogajewski, M. Bartos, J. Wyzula, D. Vaclavkova, P. Kossacki, and M. Potemski, Orbital, Spin and valley contributions to Zeeman splitting of excitonic resonances in $MoSe_2$, WSe_2 and WS_2 monolayers, 2D Mater. **6**, 015001 (2018).

[74] M. Zinkiewicz, A. O. Slobodeniuk, T. Kazimierczuk, P. Kapuściński, K. Oreszczuk, M. Grzeszczyk, M. Bartos, K. Nogajewski, K. Watanabe, T. Taniguchi, C. Faugeras, P. Kossacki, M. Potemski, A. Babiński, and M. R. Molas, Neutral and charged dark excitons in monolayer WS_2, Nanoscale **12**, 18153 (2020).